MR댐퍼 기반의 스마트 수동제어 시스템
Smart Passive System Based on MR Damper

조상원* 이헌재** 김춘호*** 이인원****
Cho, Sang Won Lee, Heon Jae Kim, Chun Ho Lee, In Won

ABSTRACT

MR댐퍼는 배터리 규모의 전력사용 및 작동의 신뢰성 그리고 경제성 등의 이유로 토목구조물의 진동제어를 위해서, 근래에 활발하게 연구되고 있는 진동제어 장치이다. 이러한 장점에도 불구하고 토목구조물에 많은 양의 MR댐퍼를 사용할 경우, 전력공급 및 센서 및 제어기 등을 포함하는 제어 시스템을 구축하고 유지 관리하는 것은 많은 노력을 필요로 한다. 따라서 본 논문에서는 전자기유도 시스템(Electromagnetic Induction System, 이하 EMI시스템)을 갖는 MR댐퍼를 제안하였다. EMI시스템은 솔레노이드 코일과 영구자석으로 구성되며, 패러데이의 전자기 유도법칙에 의해 MR댐퍼의 왕복운동을 전기에너지로 변환한다. 이렇게 생성된 전기에너지는 다시 MR댐퍼의 점성을 변화시키는 전원으로 사용되며, 생성되는 전기에너지의 강도는 MR댐퍼의 왕복운동 속도 및 영구자석의 크기 그리고 솔레노이드 코일의 회전수에 비례한다. 이러한 EMI시스템을 갖는 MR댐퍼는 전력 및 센서 그리고 제어기를 필요로 하지 않는다. 수치해석을 통해서, 기존의 MR댐퍼 시스템과의 비교하여, 제안된 EMI시스템을 갖는 MR댐퍼의 효율성을 검증하였다.

1. Introduction

Magnetorheological (MR) dampers are one of the semi-active control devices, which use MR fluids to provide controllable damping forces. Since B.F. Spencer first introduced MR dampers to civil engineering applications in mid 1990s, MR dampers have received considerable attention, because of its mechanical simplicity, high dynamic range, low operating power requirements, large force capacity, and environmental robustness. In 2001, a MR damper was applied to the cable-stayed Dongting Lake Bridge in China and the Nihon-Kagaku-Miraikan

* 한국과학기술원 토목환경공학과, 박사
** 한국과학기술원 토목환경공학과, 박사과정
*** 정회원 · 충부대학교 토목공학과, 교수
**** 정회원 · 한국과학기술원 토목환경공학과, 교수

building in Japan for reduction of responses of the structures, which are the worlds first full-scale implementations in civil engineering structures.

To reduce the responses of controlled structure, a MR damper needs a control system including a power supply such as a battery and a controller to determine the control commands using the measured responses from sensors. However, it is not easy to apply the MR damper-based control system to large-scale civil structures such as cable-stayed brides and high-rise buildings. In those cases, many MR dampers are used and each MR damper is connected to one or more power supplies and controllers. Also, many sensors are needed to measure the structural responses to determine the control commands for each MR damper. Therefore, it is difficult to build up and maintain the MR damper-based control system, especially when it is used for large-scale civil structures.

In this paper, an electromagnetic induction (EMI) system is newly adopted to MR dampers to replace a control system including a power supply, a controller, and sensors. The EMI system consists of a permanent magnet and a coil. According to the Faradays law of induction (Reitz et. al. 1993), the EMI system changes kinetic energy of reciprocation motion of the MR damper to electric energy and then electric energy is used to change the damping characteristics of MR fluid. In addition, fast motions of the MR damper induce high current and slow relative motions induce low current at the EMI system, which can adapt MR damper to the various external excitations like earthquakes. In brief, MR damper is powered and controlled by the EMI system. Therefore, the proposed MR damper with the EMI system is easy to build up and maintain, because it does not require any power supply, controller and sensors. This is an important benefit of using the MR damper with the EMI system. An EMI system was adopted to control an engine mount of the vehicle (Korea patent 2000-004066) and to control an electrorheological (ER) damper (Japan patent 2-145337). Also, we have a Korea patent(patent no. 0416398) about civil engineering application. This paper focuses on civil engineering applications of the MR damper with the EMI system. To investigate the achievable capabilities of the proposed MR damper with the EMI system, the EMI system is designed. Then, the effectiveness of performances are evaluated and compared with those of a normal MR damper system using the clipped-optimal controller.

2. MR Damper with the EMI System

A prototype MR damper has been considered to show the schematic of MR dampers, which was obtained for evaluation from the Lord Corporation and was used by Dyke et al.(1996a). As shown in Fig. 1, the magnetic field produced in the device is generated by a small electromagnet in the piston head. The current for the electromagnet is supplied by a power supply such as a battery and regulated by a controller which determines control commands, resulting in changes of damping characteristics of MR fluid. Thus, to reduce the structural

responses, the MR damper needs a control system that consists of a power supply, a controller, and sensors. When many MR dampers are used for civil engineering structures such as cable-stayed bridges and high-rise buildings, the MR damper-based control system becomes more complicated to build up and maintain.

In this paper, an electromagnetic induction (EMI) system is newly adopted to MR dampers to replace a control system. Fig. 2 shows the MR damper with the EMI system that consists of a permanent magnet and a coil. The EMI system changes kinetic energy of reciprocation motion of MR damper to electric energy according to the Faraday"s law of induction (Reitz et. al. 1993) and then electric energy is used to change the damping characteristics of MR damper. The characteristics of MR fluid is affected by magnetic field. The magnetic fields at coil 1 solidify MR fluid resulting increase of damping capacity of damper. The magnetic field is arisen by induced current of the EMI system (consists of permanent magnet and coil 2). Fast relative motions between permanent magnet and coil 2 make high current at coil 1. Slow relative motions between permanent magnet and coil 2 make low current at coil 1. Thus, MR damper with the EMI system is able to reduce the vibrations of structures by itself without any power supply and controller.

Faraday's law of induction is

$$\epsilon = -NA\frac{dB}{dt} \tag{1}$$

where ϵ is induced electromotive force(emf) that has unit of volt(V), N is number of turns of coil, B is magnetic field, and A is area of cross section.

Faraday's law of induction states that the induced emf in a closed loop equals the negative of the time rate of change of magnetic flux through the loop. External loads such as earthquakes and winds cause the reciprocal motion of MR damper. In consequence, the coil in the EMI system at the end of the piston-axle moves back and forth inducing the emf. Thus, the faster MR damper moves, the higher emf is induced and the slower MR damper moves, the lower emf is induced. This induced emf is carried to an electromagnet in the piston head and generates magnetic field around electromagnet that changes damping characteristics of MR fluid.

The proposed MR damper with the EMI system does not need sensors that measure structural responses for a controller, because the damping characteristics of MR damper is automatically regulated in proportion to the time rate of change of magnetic flux. Also, the power for electromagnet in piston head is supplied by induced emf of the EMI system, which means there is no need of a power supply. Therefore, the proposed MR damper with the EMI system can replace a conventional MR damper-based control system. This is the important benefit of using MR damper with the EMI system.

3. Analytical Model and Design

3.1. Analytical Model

The performances of the MR damper with the EMI system are now evaluated through simulations. A model of a three-story building configured with a single MR damper is considered here for direct comparisons with the normal MR damper, which is the exact one used by Dyke et al. (1996a). The MR damper is rigidly connected between the ground and the first floor of the structure.

The governing equations of the structure are given by

$$\dot{z} = Az + Bf + E\ddot{x}_g \tag{2}$$

where $\ddot{x}_g$ is a one-dimensional ground acceleration, f is the measured force generated between the structure and the MR damper, z is the state vector. The equations governing the force f predicted by this model were given by Spencer et al. (1997a).

3.2. Designing the EMI System

According to the Faraday's law of induction, the induced emf is proportional to the turns of the coil and the time rate of change of magnetic flux. Thus, the amount of emf can be regulated by the turns of the coil with a fixed capacity of permanent magnet. Appropriate number of coil turns needs to be determined in the design for better performance of the MR damper with the EMI system. In the design of the EMI system for this study, the influence of two parameters is considered: S_a, the summation of peak accelerations and S_i, the summation of peak inter-drift displacements at each floor, which are normalized by uncontrolled responses, respectively. To determine the coil turns, maximum response approach (Park et al. 2003) is used for parameters S_a and S_i with three earthquakes, El Centro, Hachinohe and Kobe earthquakes.

Fig. 3(a) shows the variations of S_a for each earthquake and Fig. 3(b) is the envelope of the maximum responses of Fig. 3(a). From Fig. 3(b), we can determine the optimal coil turns, which is the minimum point of the envelope denoted by arrow. Fig. 4 is similar to Fig. 3 except that it is for S_i. Two appropriate coil turns, 2.16×10^4 and 2.6×10^4 (turns/m), are determined from the Figs. 3 and 4. Finally, an EMI system, designed for S_a, is designated EMI_{ac} and the other EMI system, designed for S_i, is called EMI_{dr}.

For the comparison of the performance, a normal MR damper system using the clipped optimal controller (Dyke et al. 1996a,b) is considered. Two sets of appropriate weighting parameter, $q_a=5.0\times10^{13}$, $q_i=1.0\times10^{5}$ for S_a and $q_a=5.0\times10^{15}$, $q_i=5.0\times10^{6}$ for S_i, are determined. The clipped-optimal controller, designed for S_a, with weighting parameters q_a and q_i, is designated CO_{ac} and the other, designed for S_i, is called CO_{dr}.

4. Numerical Simulation Results

To verify the effectiveness of the proposed MR damper with the EMI system, a set of simulations is performed for the four historical earthquakes such as El Centro, Hachinohe, Kobe, and Northridge earthquakes. The Northridge earthquake is not considered in the designing phase, but is included here to check the validation of the design of the EMI system and the clipped-optimal controller. Simulation results of the proposed EMI system are compared to those of the normal MR damper system using the clipped optimal controller by evaluation criteria based on those used in the second generation linear control problem for buildings (Spencer et al., 1997b). The first evaluation criterion is a measure of the normalized peak floor accelerations and the inter-story drift as follows.

$$J_1 = \max_{t,i}\left(\frac{|\ddot{x}_{ai}(t)|}{\ddot{x}_a^{\max}}\right), \quad J_2 = \max_{t,i}\left(\frac{|d_i(t)|}{d_n^{\max}}\right) \tag{3}$$

where $\ddot{x}_{ai}(t)$ is the absolute accelerations of the ith floor, $\ddot{x}_a^{\max}$ is the peak uncontrolled floor acceleration, $d_i(t)$ is the inter-story drift of the above ground floors over the response history, and $d_n^{\max}$ denotes the normalized peak inter-story drift in the uncontrolled response.

Representative responses of the EMI system to four earthquakes are shown in graphs. Fig. 5 shows the velocities at the first floor where the MR damper is attached and the induced voltages by the EMI system for El Centro earthquake. For moderate earthquakes (El Centro and Hachinohe), the velocity of the first floor is smaller than that of severe earthquakes (Kobe and Northridge) with the consequence that the induced voltage by the EMI system is lower according to the Faraday"s law of induction. Also, it can be seen that the higher voltage is induced for severe earthquakes. The maximum induced voltage is 1.6V, 0.9V, 2.25V, and 2.25V for El Centro, Hachinohe, Kobe, and Northridge earthquakes, respectively, which is the voltage enough to be able to operate the MR damper. Besides, it should be noted that the induced voltage is restricted within 2.25V for the capacity of the MR damper, which is identical condition with the clipped-optimal controller. However, the induced voltage is continuously-varying whereas the command voltage of the clipped-optimal controller takes on values of either zero or the maximum value.

Table 1 shows the accelerations and the inter-story drifts at each floor for four cases of two categories (i.e., EMI_{ac}, EMI_{dr}, CO_{ac}, and CO_{dr}) normalized by each uncontrolled response, respectively. The colored cells are the minimum value among four cases at each floor. The clipped-optimal controllers achieve more reductions over the EMI systems for the moderate earthquakes such as El Centro and Hachinohe, except that the EMI systems give minimum value at the first floor. For the severe earthquakes such as Kobe and Northridge, however, the performances of the EMI system are better than those of the clipped-optimal controller giving 35.5% and 24.1% additional decreases in maximum in the peak acceleration and

inter-story drift, respectively, compared to the better clipped-optimal controller. Though the EMI system fails to achieve more reductions over the clipped-optimal controller for the moderate earthquakes, it has comparable performance to the clipped-optimal controller without the power source, controller, and sensors. This is the important benefit of using the MR damper with the EMI system.

5. Concluding Remarks

This paper has proposed the MR damper with the EMI system for a civil engineering application. The EMI system consists of a permanent magnet and a coil. According to the Faraday"s law of induction, the EMI system generates induced voltages that can supply electricity and control commands to the MR damper, replacing a normal control system such as a power supply, a controller, and sensors.

To investigate the achievable capabilities of the MR damper with the EMI system, two EMI systems were designed. Then, the effectiveness of performances are evaluated, and compared with those of a normal MR damper system. In comparing both systems, it was observed that for the moderate earthquake such as El Centro and Hachinohe, the MR damper with the EMI system showed the comparable performance to the normal MR damper system. For the severe earthquakes such as Kobe and Northridge, the MR damper with the EMI system shows the better performance giving 35.5% and 24.1% additional maximum decreases in the peak acceleration and inter-story drift, respectively.

In addition to the comparable performance, the proposed MR damper with the EMI system has the simple structure without any power supply, controller, and sensors. Therefore, the Proposed MR damper with the EMI system has potential to be implemented in real civil structures. Further studies are underway to conduct a series of experiments in which numerical simulation results will be verified.

References

1. Dyke, S.J., Spencer Jr., B.F., Sain, M.K. and Carlson, J.D., "Modeling and Control of Magnetorheological Dampers for Seismic Response Reduction," Smart Materials and Structures, Vol. 5, 1996a, pp. 565-575.
2. Dyke, S.J., Spencer Jr., B.F., Sain, M.K. and Carlson, J.D., "Seismic Response Reduction Using Magnetorheological Dampers." Proc. of the IFAC World Congress, San Francisco, CA, June 30-July 5, 1996b.
3. Reitz, J.R. Milford, F.J., and Christy R.W., Foundations of electromagnetic theory, Addison-Wesley Pub. Co, 1993.

4. Park, K.S., Jung, H.J and Lee, I.W., "Hybrid Control Strategy for Seismic Protection of a Benchmark Cable-Stayed Bridge," Engineering Structures, Vol. 25, No. 4, 2003, pp. 405-417.
5 .Spencer Jr., B.F., Dyke, S.J., Sain, M.K. and Carlson, J.D., "Phenomenological Model of a Magnetorheological Damper," J. Engrg. Mech., ASCE, Vol. 123, No. 3, 1997a, pp. 230-238.
6 .Spencer Jr., B.F., Dyke, S.J., Sain, M.K. and Carlson, J.D., "Benchmark Problems in Structural Control:-Part I: Active Mass Driver System," Proc. ASCE Struct. Congr. XV., ASCE, New York, 1997b, pp. 1265-1269.

Table 1. Normailized Peak Absolute Accelerations and Inter-Story Drifts

Story	Accelerations							
	El Centro (0.3495)*				Hachinohe (0.2294)			
	Cl-Oac	Cl-Odr	EMIac	EMIdr	Cl-Oac	Cl-Odr	EMIac	EMIdr
1st	0.499	0.551	0.355	0.340	0.492	0.515	0.372	0.377
2nd	0.354	0.433	0.436	0.396	0.431	0.520	0.526	0.530
3rd	0.441	0.473	0.512	0.492	0.384	0.465	0.404	0.423
Story	Kobe (0.8337)				Northridge (0.8428)			
	Cl-Oac	Cl-Odr	EMIac	EMIdr	Cl-Oac	Cl-Odr	EMIac	EMIdr
1st	0.370	0.429	0.367	0.345	0.897	0.881	0.568	0.568
2nd	0.494	0.493	0.484	0.485	0.587	0.554	0.612	0.586
3rd	0.410	0.384	0.387	0.393	0.815	0.800	0.725	0.738

Story	Inter-story Drifts							
	El Centro (0.3495)				Hachinohe (0.2294)			
	Cl-Oac	Cl-Odr	EMIac	EMIdr	Cl-Oac	Cl-Odr	EMIac	EMIdr
1st	0.228	0.212	0.168	0.180	0.295	0.243	0.178	0.194
2nd	0.423	0.448	0.476	0.457	0.289	0.319	0.357	0.355
3rd	0.441	0.473	0.512	0.492	0.384	0.465	0.404	0.423
Story	Kobe (0.8337)				Northridge (0.8428)			
	Cl-Oac	Cl-Odr	EMIac	EMIdr	Cl-Oac	Cl-Odr	EMIac	EMIdr
1st	0.348	0.308	0.293	0.301	0.563	0.473	0.359	0.382
2nd	0.456	0.442	0.428	0.435	0.859	0.846	0.827	0.835
3rd	0.410	0.384	0.387	0.393	0.815	0.800	0.725	0.738

* ( ) is peak ground acceleration (g)

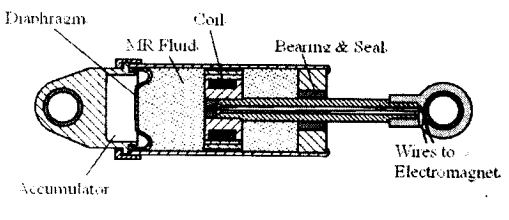

Figure 1. Schematic of a MR Damper

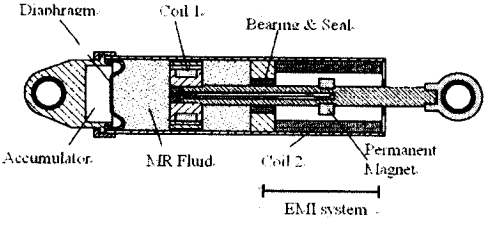

Figure 2. Schematic of a MR Damper with EMI system

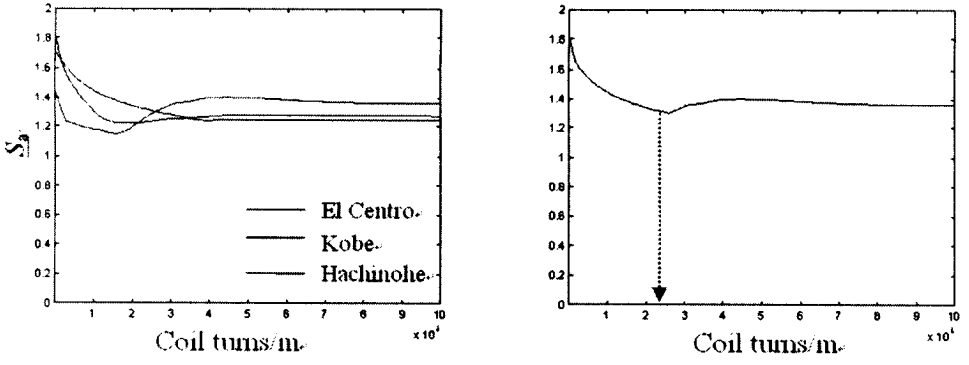

(a) Variations of S_a (b) Envelope of Max. Responses

Figure 3. Design of EMI System with S_a under Three Earthquakes

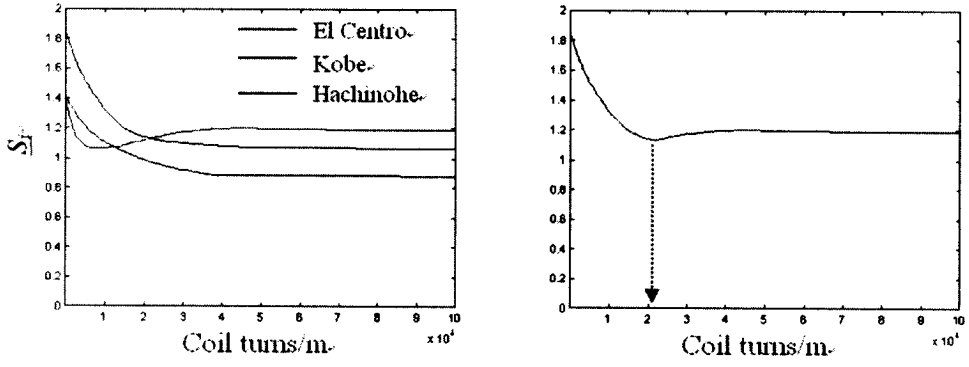

(a) Variations of S_i (b) Envelope of Max. Responses

Figure 4. Design of EMI System with S_i under Three Earthquakes

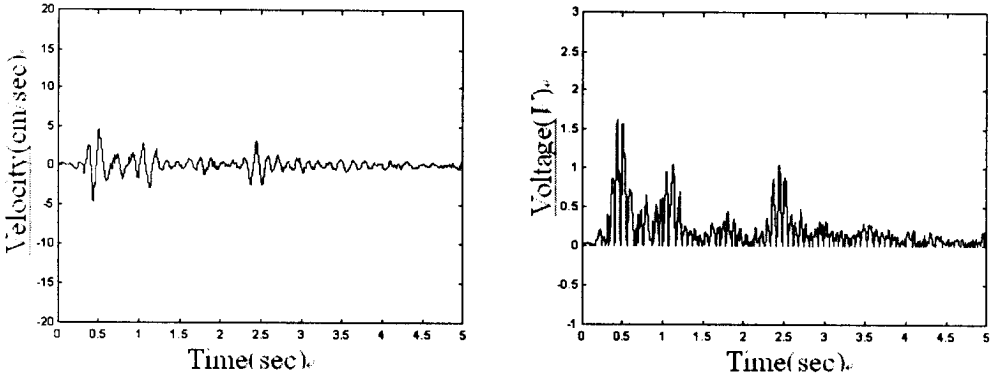

Figure 5. Velocities and Induced Voltages under El Centro Earthquake